



# The effect of pulp type on the performance of microfibrillar lignocellulosic bismuth-based active packaging material

Maisha Maliha · Rajini Brammananth ·  
Ross L. Coppel · Melissa V. Werrett ·  
Philip C. Andrews · Warren Batchelor

Received: 15 November 2021 / Accepted: 28 March 2022 / Published online: 23 April 2022  
© The Author(s) 2022

**Abstract** The study aims to investigate the effect of the different lignocellulosic pulp on the composite properties for active packaging application. Microfibrillated cellulose from bleached and unbleached Kraft and thermomechanical pulp (TMP) having different cellulose, hemicellulose, lignin, and extractive content were used as the matrix phase with antimicrobial *bis*-phosphinato bismuth complex as the dispersed phase. The Kraft pulp has thinner fibres as observed in the SEM images and have higher aspect ratio (EMT 109–157) compared to TMP (EMT 43–51). So, it is more easily fibrillated resulting in a strong close network and therefore resulting in low

water vapor transmission rate (WVTR) and high tensile index (20–91 g/m<sup>2</sup>.day and 59–78 Nm/g respectively) compared to the TMP ones (153–261 g/m<sup>2</sup>.day and 35–43 Nm/g respectively). While the physical dimension of the fibres controls the mechanical and barrier properties, the leaching and antibacterial performance is related to the bonding of the complex with the matrix. The high hydrophilicity of the bleached kraft pulp results in a weak bond with the hydrophobic bismuth complex, easing its release to kill the surrounding microbial population and thus resulting in larger zones of inhibition against both Gram-positive and Gram-negative bacteria. Therefore, bleached kraft pulp was found to be the most suitable with promising barrier, mechanical and antibacterial properties.

**Supplementary Information** The online version contains supplementary material available at <https://doi.org/10.1007/s10570-022-04562-1>.

M. Maliha · W. Batchelor (✉)  
Department of Chemical and Biological Engineering,  
Bioresource Processing Research Institute of Australia  
(BioPRIA), Monash University, VIC 3800, Australia  
e-mail: warren.batchelor@monash.edu

R. Brammananth · R. L. Coppel  
Department of Microbiology, Monash University,  
VIC 3800, Australia

M. V. Werrett · P. C. Andrews  
School of Chemistry, Monash University, VIC 3800,  
Australia

P. C. Andrews  
Centre to Impact AMR, Monash University, VIC 3800,  
Australia

**Keywords** Bismuth · Kraft · Thermomechanical ·  
Packaging · Antibacterial

## Introduction

Polymeric materials are used for packaging applications to protect the contents from contaminants and gases such as water vapour and oxygen (McKeen 2013). Conventional packaging only acts as a physical barrier, whereas antimicrobial (AM) packaging provides additional protection from microbial contamination. AM packaging helps prevent microbial growth on surfaces, thus reducing the chance of

contamination and spoilage (Appendini and Hotchkiss 2002). AM packaging can be achieved by incorporation of antimicrobial agents into the polymeric matrix.

Metal-based antimicrobial additives are becoming increasingly popular. Examples include nanoparticles, inorganic compounds and organometallic complexes of gold, silver, copper, and zinc (Patra et al. 2012). Since metal-based antimicrobials can have multiple mechanisms of action on microorganisms, it can be difficult for bacteria to develop resistance (Lemire et al. 2013; Patra et al. 2012). Due to the overuse of common antimicrobial agents, a large fraction of the bacterial population has developed some form of resistance (Pal et al. 2014). As such, there is a constant need to develop and study new antimicrobial agents. One such agent is the organometallic *bis*-phosphinato bismuth complex, [BiPh(O(O=)PPh<sub>2</sub>)<sub>2</sub>], which we have recently shown to display good antimicrobial properties (Philip et al. 2016). The complex is only sparingly soluble in water, opening up opportunities to be incorporated into materials (Werrett et al. 2018).

Active packaging materials have been studied as well as commercially used using different petroleum-based polymers such as polyethylene, ethylene, and vinyl alcohol (Oun et al. 2020; Yu et al. 2016), but recently more green and sustainable polymers have attracted considerable attention as potential replacements for these. Lignocellulosic materials are of great interest because of their biodegradability, renewability and ready availability and sources like pine needle, bagasse and rice straw are being studied by many researchers for active packaging applications (Kumar et al. 2021; Youssef et al. 2012, 2013). Microfibrillated cellulose (MFC) films are an interesting material for packaging applications, as the process of mechanical treatment to reduce fibre size substantially improves barrier and mechanical properties (Garusinghe et al. 2018). We have recently shown that MFC films loaded with the *bis*-phosphinato bismuth complex (Bi-MFC composites) can serve as high performance packaging material with antimicrobial activity towards some of the most concerning drug-resistant bacteria and fungi (Maliha et al. 2019). We have also shown that the Bi-MFC composites have antibiofilm properties, further mitigating the chances of contamination and spoilage (Maliha et al. 2021a).

Commercialisation of pure MFC products is still challenging and expensive and the current market is quite small. Bacterial cellulose and some plant sources like cotton are composed of pure cellulose and can be directly used for MFC production (Balea et al. 2020). However, most paper mills use wood-based sources to produce pulp with different compositions, containing different levels of cellulose and other components (hemicellulose, lignin, and extractives). MFC can be produced from lignocellulosic sources (Kumar et al. 2021) and thus integrating the Bi-MFC composite production into conventional pulp and paper mills can reduce production cost. Hence, this paper presents the preparation and characterisation of Bi-MFC composites using the pulp from conventional pulp and paper mills. The wood is processed to pulp in different ways in the mills to separate the fibres, either chemically (kraft, sulfite and soda pulping), mechanically or thermomechanically. The kraft process, the most common chemical pulping method, uses NaOH and Na<sub>2</sub>S to break the bonds among the cellulose, hemicellulose and lignin, getting rid of most of the lignin (Biermann 1996). A published analysis of bleached kraft pulp revealed it contained 79% cellulose and 18% hemicellulose, and very small amounts of lignin, extractives and ash (Ang et al. 2020). Bleached kraft pulp is the most commonly used pulp for MFC production (Jonoobi et al. 2015) or for preparation of MFC films and composites (Bideau et al. 2016; Dankovich and Gray 2011; Krol et al. 2015; Yan et al. 2016). Thermomechanical pulping uses heat and mechanical refining to soften the lignin to separate the fibres but does not remove the lignin, leaving approximately 30% lignin (Ma et al. 2012). There are limited studies using thermomechanical pulp (TMP) for antimicrobial composites, and so the effect of such pulp on the film properties for active packaging is not understood. In fact, only a few studies have investigated the use of TMP for MFC production (Gunawardhana et al. 2017).

The treated wood pulp fibres are often bleached, using chlorine-based chemicals, hydrogen peroxide or other bleaching agents, to increase their brightness for papermaking. Bleaching of chemical pulp removes the residual lignin to whiten the pulp. The removal of lignin increases the fibre–fibre bonding. Bleaching mechanical pulp involves a very different approach. The large amounts of lignin present are not removed, but the chromophores (part of the lignin molecule

responsible for the colour) are altered by redox reactions. Paper from thermomechanical treatment is usually used for newspapers, which can yellow as they age due to production of new chromophores from the lignin present there (Biermann 1996). Moreover, the source of fibres also plays an important role since softwood and hardwood differ in physical dimensions. Softwood fibres are longer and thicker compared to hardwood fibres and so are harder to fibrillate (Chauhan et al. 2011). Composites from natural fibres have different properties, depending on the type and content of fibre, fibre orientation, porosity, and hydrophilicity which is determined by the feedstock source and pulping process involved (Huber et al. 2012; Pickering et al. 2016). Herein, composites were made with MFC from different pulp type and sources as the matrix phase and the antimicrobial organobismuth complex was used as the dispersed phase. Figure 1 shows the sources and types of pulp studied herein describing where they are obtained from in a paper mill. The aim of the study was to characterise bismuth phosphinato loaded MFC composites and understand the effect of the carrier matrix on its properties for packaging applications.

## Methodology

### Materials

Bleached eucalyptus kraft pulp (BEK) was obtained from Australian Paper, Maryvale, Australia. Bleached (BPK) and unbleached (UPK) Radiata pine kraft pulp were obtained from Oji Fibre Solutions, New Zealand. The bleached (BTMP) and unbleached (UTMP) Radiata Pine

thermomechanical pulp were obtained from Norske Skog, Australia. The *bis*-phosphinato bismuth complex was prepared as described in our previous works (Maliha et al. 2019; Werrett et al. 2018). In brief, diphenyl phosphinic acid and triphenyl bismuth were heated under reflux for 24 h and the complex was then separated from the reaction mixture as dry powder.

### Preparation of the films

The different types of pulp were subjected to mechanical treatment using PFI mill refiner. The pulp was diluted to 10 wt% and was then subjected to 20,000 PFI mill refining revolutions. The fibres were then diluted to 1.2wt% and disintegrated in a 3L Mavis standard disintegrator (Model 8522) for 15,000 revolutions. The stock suspension was diluted to 0.2 wt% with either deionised water or Bi-complex and water suspension to make blank films or Bi-loaded composite films respectively. The Bi-complex suspension was prepared by suspending a known mass of bismuth complex in deionised water and subjected to high speed dispermat at 2000 rpm for 1 h. The amount of bismuth complex in the suspension was determined to achieve a target loading of 1% Bi complex (g of Bi-complex/g composite film). The pulp suspensions were then made into films of target basis weight of 60 g/m<sup>2</sup> using the British Handsheet Maker according to the TAPPI standard T205. Films were prepared by pouring the suspension into the handsheet maker over filter paper (GE Whatman 541 Hardened Ashless filter paper) on top of the 150-mesh screen.

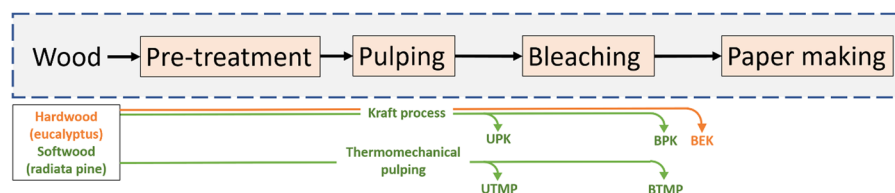


**Fig. 1** Representation of the sources and types of the pulp used for Bi-MFC composites preparation. The dashed box shows the simplified flowchart of the major processes in paper mills. The green and the orange arrows show the preparation of softwood and hardwood pulp respectively. Here the acronyms

UPK, BPK, BEK, UTMP and BTMP stands for unbleached pine kraft pulp, bleached pine kraft pulp, bleached eucalyptus kraft pulp, unbleached thermomechanical pulp and bleached thermomechanical pulp respectively

## Characterisation

### *Basis weight, thickness, and density*

The basis weight of the film was determined by measuring the dried weight of a known area of sample and dividing the weight by the area. The thickness of the films was measured using an L&W thickness tester and expressed as an average of 7 points from 3 different films and expressed as mean  $\pm$  st. dev. The density is calculated by dividing the basis weight by the thickness.

### *SEM characterisation*

The composites were cut into small pieces and mounted on a metal stub. The sample was secured using carbon tape and sputter coated with iridium metal. Scanning electron microscope (SEM) imaging of the coated samples were then done using FEI Magellan 400 FEGSEM.

### *Surface characterisation*

The surface of the blank films was studied using an OLS 5000 optical profilometer (Olympus Corporation). A height profile was analysed using the Analysis application software supplied with the instrument at the centre line of the 2D image.

### *Aspect ratio measurement*

The aspect ratio of the refined fibres were determined using the gel-point measurement method as described in Varanasi et al. (Varanasi et al. 2013). MFC suspensions of different solid concentrations ranging from 0.01 to 0.1 wt% were poured into measuring cylinders and allowed to sediment for 48 h. The initial height of the suspension ( $h_0$ ) and the final sedimentation height ( $h_s$ ) were measured. The concentration vs. ratio of final to initial height ( $h_s/h_0$ ) was fitted with a smoothing spline using the Curve Fitting Tool in MATLAB (Raj et al. 2015). The gel point is the y-intercept of its first derivative curve. The Effective Medium Theory (EMT) and Crowding Number (CN) empirical equations were then used to determine the aspect ratio.

### *FTIR analysis*

FTIR analysis was carried out using an Agilent Technologies Cary 630 ATR-FTIR (Attenuated total reflectance-Fourier Transform Infrared) spectrophotometer. The samples were placed on the diamond and scans at  $4\text{ cm}^{-1}$  in the range of  $4000\text{--}800\text{ cm}^{-1}$  were done.

### *ICP-OES analysis*

To quantify the amount of the bismuth complex in the composite films, ICP-OES (Inductively coupled plasma- optical emission spectroscopy) analysis was performed. Known mass of the films (10–20 mg) were ashed in a muffle furnace where the temperature was ramped from 25 to 600 °C over 3 h and maintained at 600 °C for an additional three hours. The ash was then dissolved in nitric acid and the amount of bismuth dissolved in the acid was then analysed using ICP-OES. This was then calculated to quantify the amount of the complex per gram of the composite films.

### *Antibacterial properties*

The antibacterial activity of the films was analysed using the Gram-positive strains *Staphylococcus aureus* (A134/ATCC 6538) and MRSA (M118797, methicillin-resistant *Staphylococcus aureus*) and the Gram-negative strains *Escherichia coli* (G102), and *Acinetobacter baumannii* (C403/ATCC17978). LB (Luria–Bertani) agar plate was used for all bacteria except for *S. aureus*, for which nutrient agar plate was used. Agar plates were spread with 20  $\mu\text{L}$  of overnight culture of a specific bacterium and 6 mm discs of the film was placed on the agar plate. The plates were incubated at 37 °C for 24 h and the zone of inhibition was measured. For each type of pulp, blank films (no bismuth) were tested as the control. Each experiment was repeated three times.

The overtime effectiveness study was performed for a specific bacterium, *S. aureus*, for 5 days. Herein, the experiment was performed the same way as mentioned above. After 24 h incubation of the plate, the discs were transferred using a sterile tweezer to a new agar plate freshly spread with the same bacterial strain. The plates were then incubated for 24 h to measure the zone of inhibition formed on day 2. This

was repeated until 5 days total incubation time was reached.

### Release behaviour

The release behaviour was studied by suspending 5 circles of the composites of 6 mm diameter in 10 mL of Milli-Q water contained in a falcon tube. The tubes were kept in an incubator shaker at 25 °C at 150 rpm for 24 h. The water was then analysed using ICP-MS (Inductively coupled plasma- mass spectroscopy).

### Water vapor transmission rate

The water vapor transmission rate (WVTR) was studied using ASTM E96 desiccant method. Standard cups containing the desiccant were sealed with the sample and incubated at 23 °C and 50% relative humidity. Weight of the cups were recorded at regular intervals and the loss in mass was plotted as a function of time. The rate of change of mass obtained from the slope was used to calculate the water vapor transmission rate.

### Mechanical properties

The mechanical properties of the films were determined using Instron Tensile Tester (Model 5965). The samples were cut into 15 mm wide strips and conditioned for 24 h at 23 °C and 50% relative humidity. 50 mm span was tested using a constant strain rate of 10 mm/min. The results were presented as an average of six replicates.

## Results and discussion

### Visual observation

Figure 2 shows the physical appearance of the composites. It can be seen that the bleached composites are whiter compared to unbleached counterparts (BPK vs UPK and BTMP vs. UTMP), as expected. Bleached kraft pulp from both the softwood (BPK) and hardwood (BEK) looked similar. However, the bleached thermomechanical pulp film (BTMP) is yellower, which is due to its higher lignin content. As expected, the pulping method and the bleaching step

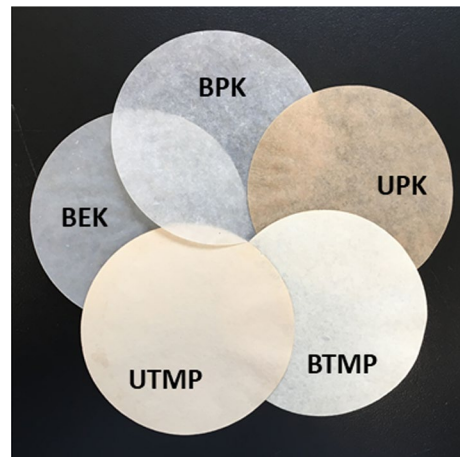


**Fig. 2** Physical appearance of the composites using bleached eucalyptus kraft pulp (BEK), bleached (BPK) and unbleached (UPK) radiata pine kraft pulp and bleached (BTMP) and unbleached (UTMP) radiata pine thermomechanical pulp

has a significant influence on the appearance of the composites.

### Characterisation

#### *Basis weight, thickness, and density*

#### *SEM characterisation*

Figure 3 shows the secondary electron images of the composites prepared from the different kinds of pulp. Herein, it is clearly seen that the composites from the kraft pulp (BEK, BPK, UPK) are composed of significantly thinner fibres compared to the thermomechanical pulp (BTMP, UTMP). The kraft pulp films consist of a closely arranged network of mostly very thin fibres with a few thicker fibre bundles. The thermomechanical films, on the other hand, are made up of thick bundles of fibres forming an open and more porous network. Spence et al. reported that kraft pulp produces fibres in nanometre range, but the same fibrillation treatment resulted in TMP fibres in micron scale. Unrefined fibres from both bleached and unbleached softwood pulp were reported to be around 30 µm, bleached and unbleached hardwood pulp to be 20 µm, and TMP to be 34 µm (Spence et al. 2010). The secondary electron images give an understanding of the

**Table 1** Average aspect ratio values calculated from the gel point determined using the EMT and CN empirical equations

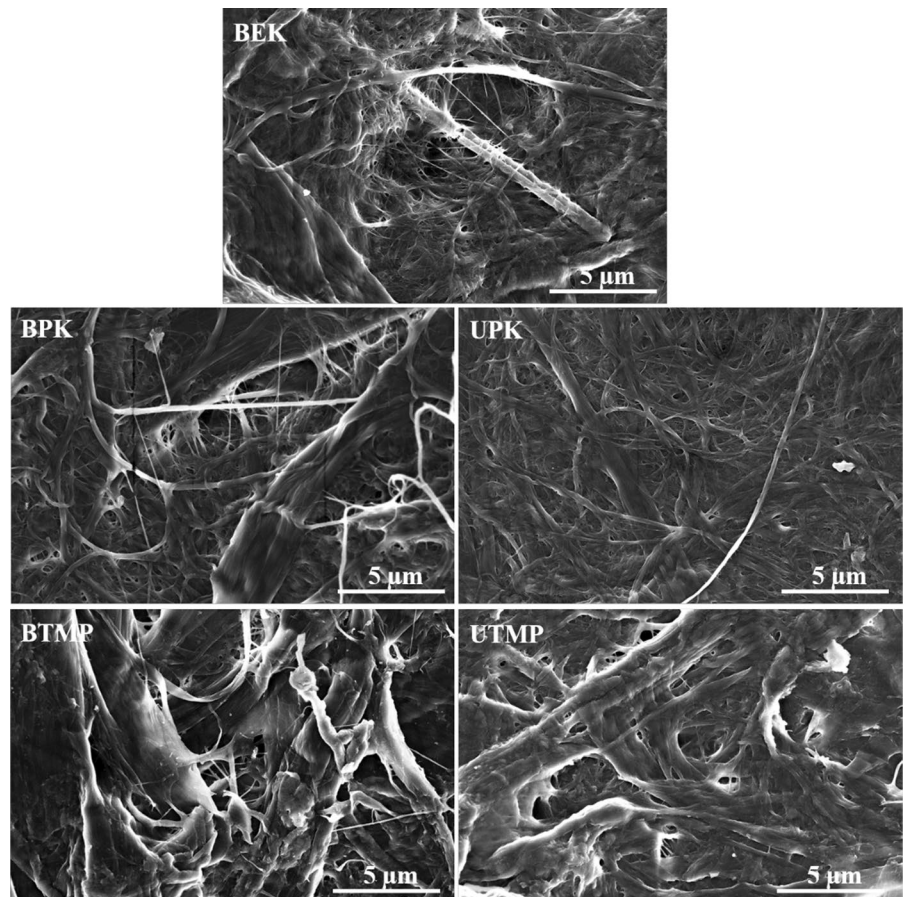
Type of pulp	Gel point, $C_c$ (wt%)	Aspect ratio	
		EMT	CN
BEK	0.222	109	127
BPK	0.150	137	155
UPK	0.119	157	174
BTMP	1.110	43	57
UTMP	0.824	51	66

fibre dimensions to better understand the film properties. The back-scattered electron (BSE) images in figure S1 shows that the bismuth complex (shown as bright structures) is distributed throughout the material in all the composites.

### Surface characterisation

Figure 4 shows the optical profilometry images of the surface of the blank films and their height profiles. The height profile of the images on the horizontal centre line (white dashed line) shows that the bleached and unbleached thermomechanical pulp films demonstrate more variation in height. The height variation of BEK, BPK and UPK does not exceed 15  $\mu\text{m}$ , whereas BTMP and UTMP surfaces show height up to 20 and 25  $\mu\text{m}$  respectively. The larger difference in height in the TMP films is due to the presence of thick fibres giving rise to a rougher surface. While the SEM images provide higher resolution micrographs with qualitative information about the fibre size, the height data in the profilometry images gives a good understanding about the surface topography of the films over a larger area.

**Fig. 3** Micrographs of the composite films from bleached eucalyptus kraft pulp (BEK) (top), bleached (BPK) and unbleached (UPK) radiata pine kraft pulp (middle panel), bleached (BTMP) and unbleached (UTMP) radiata pine thermomechanical pulp (bottom panel) showing the fibre dimensions



### Aspect ratio

Table 1 shows the aspect ratios of the fibres studied using the EMT and CN theories. It is clear that the kraft pulp (BEK, BPK, UPK) have lower gel points and higher aspect ratios compared to the thermomechanical pulp (BTMP and UTMP). The gel point is the lowest concentration at which the fibres in the suspension can form a continuous network and the aspect ratio is the ratio of length to diameter of each of the fibres, both giving us an indication of the fibre dimensions. The kraft pulp has a significantly higher aspect ratio, indicating they are much easier to fibrillate. A similar result was also reported by Peltola et al. (Peltola et al. 2011). On the other hand, the aspect ratio for TMP is quite low. Gunawardhana et al. reported that TMP is much less responsive to fibrillation treatment and even energy-intensive treatments of up to 200,000 kWh/tonne fibre can only change the aspect ratio to 120 approximately and reduce the fibre diameter to 40 nm (Gunawardhana et al. 2017). In comparison, with BEK a fibrillation treatment of only 3542 kWh/tonne is sufficient to achieve an aspect ratio of 102 and fibre diameter of 31 nm. In fact, 40,000 kWh/tonne will result in aspect ratio and fibre diameter of 229 and 12 nm respectively (Ang et al. 2019). In this paper, the refining treatment is equivalent to 7000 kWh/tonne fibre. Softwood fibres are longer than hardwood fibres (Chauhan et al. 2011), which could be the reason behind the slightly higher aspect ratio of BPK than BEK.

### FTIR analysis

Figure 5 shows the FTIR spectra of the bismuth complex loaded composite films prepared using the different kinds of pulp. FTIR analysis of both the blank and Bi-loaded films were performed. They do not

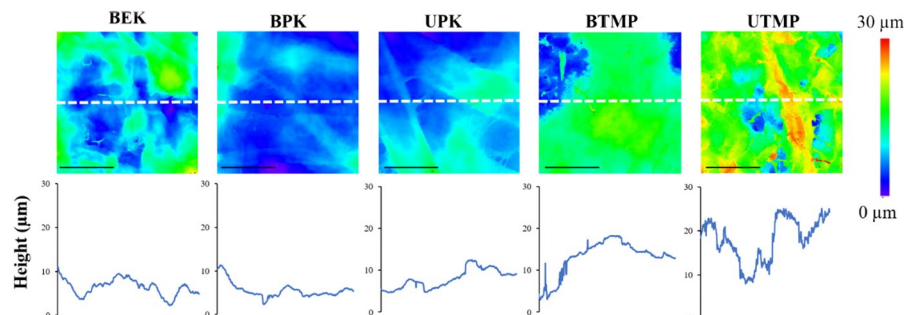
**Table 2** Actual bismuth complex content of the composite films analysed from ICP-OES analysis

Type of pulp	Actual Bi-complex content (wt%) (g of Bi complex/g composite film)
BEK	0.78 ± 0.01
BPK	0.82 ± 0.01
UPK	1.09 ± 0.19
BTMP	1.10 ± 0.03
UTMP	1.04 ± 0.03

show any change in peaks irrespective of the presence or absence of the complex since a low level of loading (1 wt%) has been studied here. Thus, the spectrum for the Bi-loaded composites only are shown in the figure for simplicity and the spectra of the blank films are shown in figure S2. There are a few strong peaks for the bleached and unbleached thermomechanically treated pulp films (BTMP and UTMP), which are missing in the kraft pulp ones. The peaks at 1510  $\text{cm}^{-1}$  (labelled as 1 in the inset plot) represent the aromaticity, at 1260  $\text{cm}^{-1}$  (labelled as 2 in the inset plot) represent the alkyl aryl group, and the peaks at 1020  $\text{cm}^{-1}$  (labelled as 3) represent the aliphatic ether in the lignin.

Thermomechanical treated pulp has around 38% cellulose and quite high lignin content of 30% approximately, along with the highest level of extractives. Bleached and unbleached kraft pulp from softwood or hardwood, on the other hand, has high cellulose content (78–79%), around 20% hemicellulose and low lignin and extractives content (Spence et al. 2010). The large amount of lignin present in the thermomechanically treated pulp is evident from the FTIR results.

**Fig. 4** Optical profilometry images of the surface of blank films (no bismuth) (top panel) and the height profiles of the surface along the horizontal centre line shown (bottom panel). The scale bars indicate 50  $\mu\text{m}$



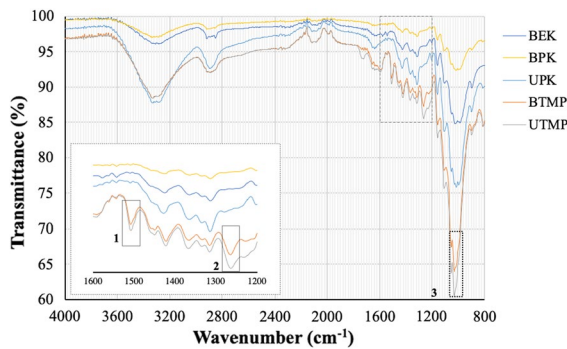


**Fig. 5** FTIR spectrum of the Bi-complex loaded films prepared from bleached eucalyptus kraft pulp (BEK), bleached (BPK) and unbleached (UPK) radiata pine kraft pulp and bleached (BTMP) and unbleached (UTMP) radiata pine thermomechanical pulp showing the difference in chemical composition

### ICP-OES analysis

Table 2 shows the actual amount of bismuth complex in the composites determined using ICP-OES analysis. It can be clearly seen that the bleached kraft pulp composites have slightly lower amounts of bismuth complex than targeted, similar to our previous work (Maliha et al. 2019). It can be speculated that the highly hydrophobic nature of the complex results in loss of the complex during preparation of the films. On the other hand, the unbleached kraft pulp and the thermomechanically treated pulp contains the targeted amount within the standard error limits. Kraft pulp has very low levels of lignin, and bleaching removes

any residual lignin. Lignin, being a complex organic polymer containing phenol groups, forms hydrophobic interactions with the bismuth complex, resulting in higher additive retention in the composites. Similarly, the lignin in the unbleached kraft pulp, although in small quantities, helps in the bismuth complex retention in the composites. The lignin-free bleached kraft pulp, containing mainly hydrophilic cellulose, does not have a hydrophobic interaction with the complex, resulting in more loss of the complex.

### Antibacterial properties

Figure 6 shows the zones of inhibition of the bismuth complex loaded composites prepared from different types of pulp. Figure 6A shows that the composites have larger zones of inhibition and appear to be more active against Gram-positive bacteria (*S. aureus*, antibiotic sensitive and resistant (MRSA strains)) compared to the Gram-negative ones (*E. coli* and *A. baumannii*). This is consistent with our previous work with bismuth complex-MFC composites (Maliha et al. 2019). Gram-negative bacteria are harder to kill due to their lipopolysaccharide membrane, which is absent in Gram-positive bacteria. Larger zones of inhibition are often thought to indicate a low minimum inhibitory concentration and hence somewhat higher relative activity, but in fact this is debatable and may be dependent on a number of other factors such as ease of diffusion (Cooper 1963). However, the complex has been shown to be selectively more active on the Gram-negative bacteria when prepared

**Table 3** Basis weight, thickness and density of the blank films and the Bi-loaded composite films from bleached eucalyptus kraft pulp (BEK), bleached (BPK) and unbleached (UPK)

radiata pine kraft pulp and bleached (BTMP) and unbleached (UTMP) radiata pine thermomechanical pulp

Source of wood	Type of pulp	Sample		Basis weight (g/m <sup>2</sup> )	Thickness (μm)	Density (g/cm <sup>3</sup> )
Hardwood (eucalyptus)	Kraft	BEK	Blank	69 ± 3	87 ± 6	0.80
			Bi-loaded	69 ± 1	85 ± 5	0.81
Softwood (radiata pine)	Kraft	BPK	Blank	62 ± 3	94 ± 7	0.66
			Bi-loaded	62 ± 3	91 ± 5	0.68
		UPK	Blank	64 ± 2	107 ± 6	0.59
			Bi-loaded	69 ± 1	107 ± 5	0.65
	Thermo-mechanical	BTMP	Blank	64 ± 2	101 ± 4	0.63
			Bi-loaded	66 ± 2	105 ± 8	0.63
		UTMP	Blank	62 ± 2	115 ± 11	0.54
			Bi-loaded	62 ± 1	120 ± 10	0.52



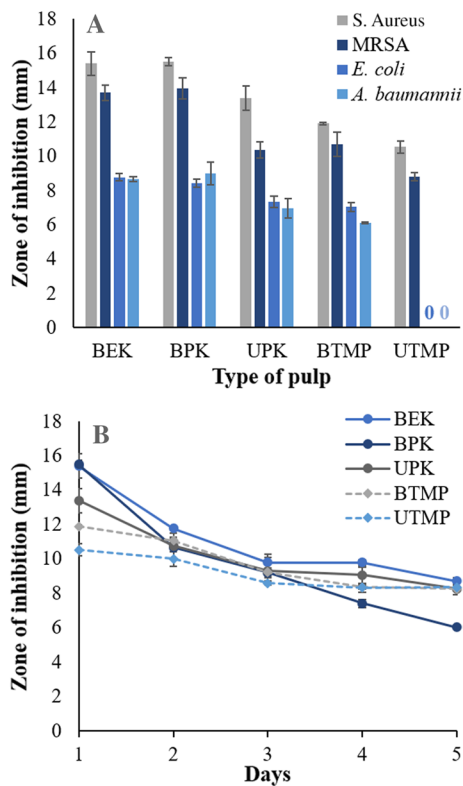


**Fig. 6** The zones of inhibition of the bismuth complex loaded composites of bleached eucalyptus kraft pulp (BEK), bleached (BPK) and unbleached (UPK) radiata pine kraft pulp and bleached (BTMP) and unbleached (UTMP) radiata pine thermomechanical pulp against different bacteria after 24 h (A) and against *S. aureus* over a period of 5 days (B). There was no zone observed where it is labelled with a zero (0) in the graph

in hydrogel form and dispersed in a bacterial broth in our previous work (Maliha et al. 2021b). This difference in behaviour from the disk diffusion test and the broth suspension is not yet understood.

The bleached kraft pulp films (both BEK and BPK) have similar, large zones of inhibition, followed by the unbleached kraft pulp and the thermomechanically treated pulps. However, the unbleached thermomechanical pulp (UTMP) composite does not inhibit the growth of either of the Gram-negative bacteria. It is interesting that although the BEK and BPK showed larger zones of inhibition, they showed a lower bismuth content than the other samples according to the ICP-OES analysis. The larger zones of inhibition for the bleached kraft pulp could potentially be due to a higher leaching ability of the bismuth complex. Figure 6B shows the antibacterial activity of

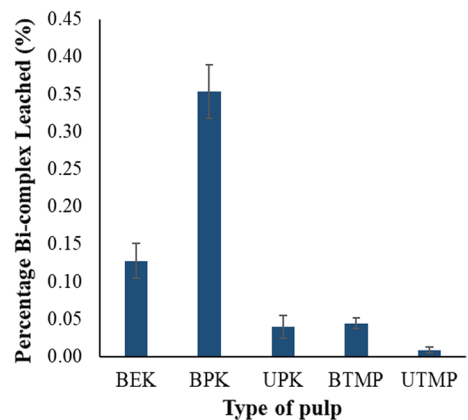


**Fig. 7** The percentage of bismuth complex released into water from composite films of bleached eucalyptus kraft pulp (BEK), bleached (BPK) and unbleached (UPK) radiata pine kraft pulp and bleached (BTMP) and unbleached (UTMP) radiata pine thermomechanical pulp. The bars represent the percentage of bismuth complex present in the leachate after 24 h with respect to the mass of the complex contained in the composites. The error bars show the standard deviation

the composites over a period of 5 days against the Gram-positive bacteria *S. aureus*. The zone of inhibition decreases with each day due to the loss of the bismuth complex that has leached out into the agar. Similar behaviour was also observed in our previous work (Maliha et al. 2019).

#### Release behaviour

Figure 7 shows the percentage of bismuth complex leached out into the water with respect to the total amount of bismuth complex present in the composites. The bleached kraft softwood pulp (BPK) shows the highest amount of complex leached into the water, followed by similarly treated hardwood pulp (BEK). The bismuth complex is a highly hydrophobic complex, and has been suggested to exist in a polymeric form (Werrett et al. 2018). It is likely that the complex is weakly bonded with the bleached kraft pulp. The kraft pulp contains mainly cellulose and hemicellulose, which are hydrophilic polymers. The complex is sustained in the matrix only by physical entrapment within the fibre network. This may also have resulted in lower loading of the bismuth complex than the loading of other composites presented in Table 2. This also explains the higher release behaviour of the complex into the agar plates resulting in relatively

larger zones of inhibition in Fig. 6. By contrast, the thermomechanical pulp contains a large amount of lignin, which forms a hydrophobic interaction with the complex. The behaviour of lignin in TMP forming higher adhesion with co-polymer PLA in composites was also reported previously (Peltola et al. 2011).

The highest leachability of BPK explains its loss of antibacterial activity over time. Lower amounts of the bismuth complex diffuse out from unbleached kraft pulp and the bleached and unbleached thermomechanical pulp. The unbleached thermomechanical pulp (UTMP) leaches the least and hence the accessibility of the complex for bacteria is reduced explaining the reduced antibacterial effectiveness. The lower accessibility of the complex in UTMP reduces its effectiveness against the hard-to-treat Gram-negative bacteria.

#### Water vapor transmission rate

Figure 8 shows the water vapor transmission rate of the films prepared from the different types of pulp. It is clear that the kraft pulp films (20–91 g/m<sup>2</sup>.day) have better barrier performance to water vapor compared to the thermomechanical films (153–261 g/m<sup>2</sup>.day). The chemically treated pulp is more easily refined and when subjected to similar refining treatments, the kraft pulp undergo more fibrillation than the thermomechanical pulp. This can be verified from

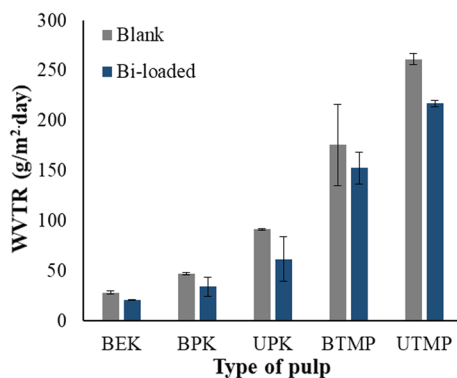


**Fig. 8** The water vapor transmission rate (WVTR) of the films prepared from bleached eucalyptus kraft pulp (BEK), bleached (BPK) and unbleached (UPK) radiata pine kraft pulp and bleached (BTMP) and unbleached (UTMP) radiata pine thermomechanical pulp with and without the bismuth complex at 23 °C and 50% relative humidity. The error bars indicate standard deviations

the SEM images showing thinner fibre diameter for the kraft pulp. The thin fibres form a dense network held together by strong hydrogen bonding. This dense network increases the tortuosity making it harder for small water vapor molecules to pass through. The strong hydrogen bonding also results in stronger films. Table 3 shows that the material density of BEK was higher compared to BPK, although both are bleached kraft pulp. The unbleached pulp films (UPK and UTMP) are less dense and thicker than their respective bleached counterparts (BPK and BTMP).

WVTR is reported to be dependent on the material density (Rojo et al. 2015), which was higher for BEK (0.80 and 0.81 g/cm<sup>3</sup>) compared to BPK (0.66 and 0.68 g/cm<sup>3</sup>), as presented in Table 3. Thus, since both BEK and BPK are bleached kraft pulp, the difference in density could be the reason for the variation in water vapor transmission rate. With decrease in density, the films have a more open network structure leading to an increased pore volume. Moreover, softwood fibres are long and thick and hardwood fibres comparatively short and thin. Thus, softwood fibres need coarser refiner plates to break them down (Chauhan et al. 2011). The fibres in BPK might not be as fibrillated as BEK which might have resulted in the variation in density and water vapor barrier performance. The films from bleached pulp (BPK and BTMP) show better barrier performance than its unbleached counterpart (UPK and UTMP). Other studies have shown that the WVTR for bleached hardwood kraft pulp, unrefined or refined using valley beater and homogeniser, is lower than the unbleached pulp (Spence et al. 2011). In our previous study, composites prepared by spraying technique showed increase in water vapor permeability on addition of the bismuth complex (Maliha et al. 2019). Interestingly herein, the addition of bismuth complex decreases the transmission rate. The large bismuth complex particles seem to fill in the pores when vacuum was applied during sheet formation. The WVTR of a common packaging material, low density polyethylene, has been reported to be in the range of 16–23 g/m<sup>2</sup>.day (Rodionova et al. 2011). The WVTR of cellulose nanofibers (CNF) and acylated CNF has been reported to be 234 g/m<sup>2</sup>.day and 167 g/m<sup>2</sup>.day respectively (Nair et al. 2014). For a packaging application, a low WVTR is desired. Thus, based on the barrier properties, the kraft pulp is a better choice for

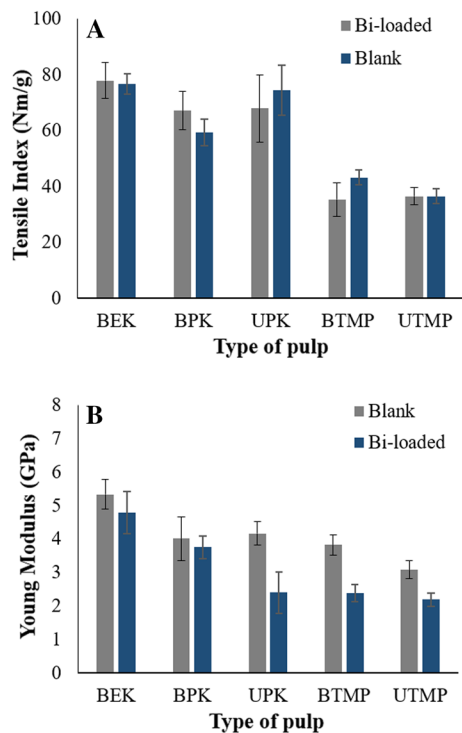


**Fig. 9** Mechanical properties from tensile testing for composite films from bleached eucalyptus kraft pulp (BEK), bleached (BPK) and unbleached (UPK) radiata pine kraft pulp and bleached (BTMP) and unbleached (UTMP) radiata pine thermomechanical pulp with and without bismuth complex loading expressed as an average tensile index (A) and Young modulus (B). Error bars represent 95% confidence interval

preparation of bismuth complex loaded packaging material.

### Mechanical properties

The mechanical properties of the films from different pulps with and without the bismuth complex are shown in Fig. 9. The films from the kraft pulp have significantly higher tensile index and thus are stronger than the films from the thermomechanical pulp. Unrefined BEK has a tensile index of 30 Nm/g (Ang et al. 2019) which has been improved to  $78 \pm 8$  Nm/g. The mechanical properties were reported to be independent of the lignin content up to 14% lignin by Rojo et al. (Rojo et al. 2015), which explains the similar mechanical properties of BPK and UPK. Beyond that level, high lignin content interferes significantly with the bonding

between fibres. Mechanical treatment results in low strength pulp nonetheless (Biermann 1996), resulting in weaker films. The presence of large amounts of lignin in TMP limits the extent of fibrillation, resulting in larger fibre diameter and thereby weak films (Spence et al. 2010). The addition of the bismuth complex does not have any detrimental effect on the tensile index of the films. However, the Young Modulus decreases implying that the films become slightly more elastic when the bismuth complex is present.

### Conclusion

This paper optimises the most suitable type of lignocellulosic matrix for active packaging applications. The performance of the composite material is determined by two controlling factors, the interaction of the bismuth complex with the matrix phase and the physical dimensions of the fibres. While the leaching properties and the antibacterial activity is directly related to the bonding between the bismuth complex and the carrier matrix, the mechanical and barrier properties are linked to the extent of fibrillation. The weak interaction of the complex with the hydrophilic matrix in the bleached kraft pulp composites makes it more available to be released and kill the bacteria in the surrounding environment. The kraft pulps are most easily fibrillated and so produced the lowest diameter fibres, when refined to the same extent. This results in a more compact structure with strong hydrogen bond, resulting in lower water vapor transmission rate and high tensile strength (20–91  $\text{g/m}^2\cdot\text{day}$  and 59–78 Nm/g respectively) compared to the TMP ones (153–261  $\text{g/m}^2\cdot\text{day}$  and 35–43 Nm/g respectively). Thus, the bleached kraft pulp appears to be a great choice in terms of barrier performance, mechanical properties, and antibacterial properties. Hardwood or softwood does not make a significant difference in the composite properties for packaging applications. The presence of the bismuth complex improves the barrier performance and does not have any significant detrimental effect on the tensile index. Thus, the bismuth complex can be used as the antibacterial agent in such lignocellulosic active packaging material. This paper provides a good understanding of the material performance using the different kinds of pulp that is

available in the paper mills to help choose the best carrier matrix for the complex to translate the active packaging material production in paper mills.

**Acknowledgments** The authors acknowledge the financial support from Monash University and The National Health and Medical Research Council (APP1139844). The authors would like to acknowledge the use of the facilities in the Monash Centre for Electron Microscopy. The authors would like to thank Dr. Thilina Gunawardhana for his assistance in obtaining the pulp from different mills. Maisha Maliha would like to acknowledge the Australian Government for the Research Training Program (RTP) Scholarship.

**Author contributions** Conceptualization: MM, MW, PA, WB; Methodology: MM; Investigation: MM, RB, MW; Formal analysis: MM; Writing—original draft preparation: MM; Writing—review and editing: MM, RB, RLC, MW, PCA, WB; Funding acquisition: WB; Resources: RLC, PCA, WB; Supervision: MW, PCA, WB.

**Funding** Open Access funding enabled and organized by CAUL and its Member Institutions. The National Health and Medical Research Council (APP1139844).

#### Declarations

**Conflict of interest** There are no conflicts of interest to declare.

**Open Access** This article is licensed under a Creative Commons Attribution 4.0 International License, which permits use, sharing, adaptation, distribution and reproduction in any medium or format, as long as you give appropriate credit to the original author(s) and the source, provide a link to the Creative Commons licence, and indicate if changes were made. The images or other third party material in this article are included in the article's Creative Commons licence, unless indicated otherwise in a credit line to the material. If material is not included in the article's Creative Commons licence and your intended use is not permitted by statutory regulation or exceeds the permitted use, you will need to obtain permission directly from the copyright holder. To view a copy of this licence, visit <http://creativecommons.org/licenses/by/4.0/>.

#### References

- Ang S, Haritos V, Batchelor W (2019) Effect of refining and homogenization on nanocellulose fiber development, sheet strength and energy consumption. *Cellulose* 26(8):4767–4786. <https://doi.org/10.1007/s10570-019-02400-5>
- Ang S, Haritos V, Batchelor W (2020) Cellulose nanofibers from recycled and virgin wood pulp: a comparative study of fiber development. *Carbohydr Polym* 234:115900–115900. <https://doi.org/10.1016/j.carbpol.2020.115900>
- Appendini P, Hotchkiss JH (2002) Review of antimicrobial food packaging. *Innov Food Sci Emerg Technol* 3(2):113–126. [https://doi.org/10.1016/S1466-8564\(02\)00012-7](https://doi.org/10.1016/S1466-8564(02)00012-7)

- Balea A, Fuente E, Monte MC, Merayo N, Campano C, Negro C, Blanco A (2020) Industrial application of nanocelluloses in papermaking: a review of challenges, technical solutions, and market perspectives. *Molecules* 25(3):526. <https://doi.org/10.3390/molecules25030526>
- Bideau B, Bras J, Saini S, Daneault C, Loranger E (2016) Mechanical and antibacterial properties of a nanocellulose-polypyrrole multilayer composite. *Mater Sci Eng C Mater Biol Appl* 69:977–984. <https://doi.org/10.1016/j.msec.2016.08.005>
- Biermann CJ (1996) *Handbook of Pulping and Papermaking*. Elsevier Science & Technology, San Diego
- Chauhan VS, Kumar N, Kumar M, Chakrabarti SK, Thapar SK (2011) Effect of separate and mixed refining of hardwood and softwood pulps on paper properties. *J Korea Tech Assoc Pulp Paper Indus* 43(4):1–10
- Cooper KE (1963) Chapter 1 - The theory of antibiotic inhibition zones. In: Kavanagh F (ed) *Analytical microbiology*. Academic Press, pp 1–86. <https://doi.org/10.1016/B978-1-4832-3129-7.50037-3>
- Dankovich TA, Gray DG (2011) Bactericidal paper impregnated with silver nanoparticles for point-of-use water treatment. *Environ Sci Technol* 45(5):1992–1998. <https://doi.org/10.1021/es103302t>
- Garusinghe UM, Varanasi S, Raghuwansi VS, Garnier G, Batchelor W (2018) Nanocellulose-montmorillonite composites of low water vapour permeability. *Colloids Surf, A* 540:233–241. <https://doi.org/10.1016/j.colsurfa.2018.01.010>
- Gunawardhana T, Raj P, Varanasi S, Garnier G, Patti A, Batchelor W (2017) Development of cellulose nanofibre quality with mechanical energy: effect of starting material. In: 16th Fundamental Research Symposium. Oxford
- Huber T, Müssig J, Curnow O, Pang S, Bickerton S, Staiger MP (2012) A critical review of all-cellulose composites. *J Mater Sci* 47(3):1171–1186. <https://doi.org/10.1007/s10853-011-5774-3>
- Jonoobi M, Oladi R, Davoudpour Y, Oksman K, Dufresne A, Hamzeh Y, Davoodi R (2015) Different preparation methods and properties of nanostructured cellulose from various natural resources and residues: a review. *Cellulose* 22(2):935–969. <https://doi.org/10.1007/s10570-015-0551-0>
- Krol LF, Beneventi D, Alloin F, Chaussy D (2015) Microfibrillated cellulose-SiO<sub>2</sub> composite nanopapers produced by spray deposition. *J Mater Sci* 50(11):4095–4103. <https://doi.org/10.1007/s10853-015-8965-5>
- Kumar A, Gupta V, Gaikwad KK (2021) Microfibrillated cellulose from pine cone: extraction, properties, and characterization. *Biomass Convers Bioref*. <https://doi.org/10.1007/s13399-021-01794-2>
- Kumar A, Gupta V, Singh S, Saini S, Gaikwad KK (2021) Pine needles lignocellulosic ethylene scavenging paper impregnated with nanozeolite for active packaging applications. *Indus Crops Prod* 170:113752. <https://doi.org/10.1016/j.indcrop.2021b.113752>
- Lemire JA, Harrison JJ, Turner RJ (2013) Antimicrobial activity of metals: mechanisms, molecular targets and applications [Review Article]. *Nature Rev Microbiol* 11:371. <https://doi.org/10.1038/nrmicro3028>. <https://www.nature.com/articles/nrmicro3028#supplementary-information>

- Ma P, Fu S, Zhai H, Law K, Daneault C (2012) Influence of TEMPO-mediated oxidation on the lignin of thermomechanical pulp. *Bioresour Technol* 118:607–610. <https://doi.org/10.1016/j.biortech.2012.05.037>
- Maliha M, Herdman M, Brammananth R, McDonald M, Coppel R, Werrett M, Andrews P, Batchelor W (2019) Bismuth phosphinate incorporated nanocellulose sheets with antimicrobial and barrier properties for packaging applications. *J Clean Prod*. <https://doi.org/10.1016/j.jclepro.2019.119016>
- Maliha M, Brammananth R, Dyson J, Coppel RL, Werrett M, Andrews PC, Batchelor W (2021a) Biocompatibility and selective antibacterial activity of a bismuth phosphinato-nanocellulose hydrogel. *Cellulose*. <https://doi.org/10.1007/s10570-021-03835-5>
- Maliha M, Tan B, Wong K, Miri S, Brammananth R, Coppel RL, Werrett M, Andrews PC, Batchelor W (2021b) Bismuth phosphinato incorporated antibacterial filter paper for drinking water disinfection. *Coll Surf A: Physicochem Eng Aspects* 627:127167. <https://doi.org/10.1016/j.colsurfa.2021b.127167>
- McKeen LW (2013) Introduction to use of plastics in food packaging. In: *Plastic films in food packaging*. William Andrew Publishing, pp 1–15. <https://doi.org/10.1016/B978-1-4557-3112-1.00001-6>
- Nair SS, Zhu JY, Deng Y, Ragauskas AJ (2014) High performance green barriers based on nanocellulose. *Sustain Chem Process* 2(1):23. <https://doi.org/10.1186/s40508-014-0023-0>
- Oun AA, Shankar S, Rhim JW (2020) Multifunctional nanocellulose/metal and metal oxide nanoparticle hybrid nanomaterials. *Crit Rev Food Sci Nutr* 60(3):435–460. <https://doi.org/10.1080/10408398.2018.1536966>
- Pal C, Bengtsson-Palme J, Rensing C, Kristiansson E, Larsson DGJ (2014) BacMet: antibacterial biocide and metal resistance genes database. *Nucleic Acids Res* 42:D737. <https://doi.org/10.1093/nar/gkt1252>
- Patra M, Gasser G, Metzler-Nolte N (2012) Small organometallic compounds as antibacterial agents. *Dalton Trans* 41(21):6350–6358. <https://doi.org/10.1039/C2DT12460B>
- Peltola H, Laatikainen E, Jetsu P (2011) Effects of physical treatment of wood fibres on fibre morphology and biocomposite properties. *Plast, Rubber Compos* 40(2):86–92. <https://doi.org/10.1179/174328911X12988622801016>
- Philip A, Werrett M, Madleen B (2016) Antibacterial bismuth complexes (Australia Patent No).
- Pickering KL, Efendy MGA, Le TM (2016) A review of recent developments in natural fibre composites and their mechanical performance. *Compos Part A: Appl Sci Manuf* 83:98–112. <https://doi.org/10.1016/j.compositesa.2015.08.038>
- Raj P, Varanasi S, Batchelor W, Garnier G (2015) Effect of cationic polyacrylamide on the processing and properties of nanocellulose films [Article]. *J Coll Interf Sci* 447:113–119. <https://doi.org/10.1016/j.jcis.2015.01.019>
- Rodionova G, Lenes M, Eriksen Ø, Gregersen Ø (2011) Surface chemical modification of microfibrillated cellulose: improvement of barrier properties for packaging applications. *Cellulose* 18(1):127–134. <https://doi.org/10.1007/s10570-010-9474-y>
- Rojo E, Peresin MS, Sampson WW, Hoeger IC, Vartiainen J, Laine J, Rojas OJ (2015) Comprehensive elucidation of the effect of residual lignin on the physical, barrier, mechanical and surface properties of nanocellulose films. *Green Chem* 17(3):1853–1866. <https://doi.org/10.1039/c4gc02398f>
- Spence KL, Venditti RA, Habibi Y, Rojas OJ, Pawlak JJ (2010) The effect of chemical composition on microfibrillar cellulose films from wood pulps: mechanical processing and physical properties. *Bioresour Technol* 101(15):5961–5968. <https://doi.org/10.1016/j.biortech.2010.02.104>
- Spence KL, Venditti RA, Rojas OJ, Habibi Y, Pawlak JJ (2011) A comparative study of energy consumption and physical properties of microfibrillated cellulose produced by different processing methods. *Cellulose* 18(4):1097–1111. <https://doi.org/10.1007/s10570-011-9533-z>
- Varanasi S, He R, Batchelor W (2013) Estimation of cellulose nanofibre aspect ratio from measurements of fibre suspension gel point. *Cellulose* 20(4):1885–1896. <https://doi.org/10.1007/s10570-013-9972-9>
- Werrett M, Herdman M, Brammananth R, Garusinghe U, Batchelor W, Crellin P, Coppel R, Andrews PC (2018) Bismuth Phosphinates in Bi-Nanocellulose composites and their efficacy towards multi-drug resistant bacteria. *Chem- A Euro J*. <https://doi.org/10.1002/chem.201801803>
- Yan J, Abdelgawad AM, El-Naggar ME, Rojas OJ (2016) Antibacterial activity of silver nanoparticles synthesized In-situ by solution spraying onto cellulose. *Carbohydr Polym* 147:500–508. <https://doi.org/10.1016/j.carbpol.2016.03.029>
- Youssef AM, El-Samahy MA, Abdel Rehim MH (2012) Preparation of conductive paper composites based on natural cellulosic fibers for packaging applications. *Carbohydr Polym* 89(4):1027–1032. <https://doi.org/10.1016/j.carbpol.2012.03.044>
- Youssef AM, Kamel S, El-Samahy MA (2013) Morphological and antibacterial properties of modified paper by PS nanocomposites for packaging applications. *Carbohydr Polym* 98(1):1166–1172. <https://doi.org/10.1016/j.carbpol.2013.06.059>
- Yu HY, Yang XY, Lu FF, Chen GY, Yao JM (2016) Fabrication of multifunctional cellulose nanocrystals/poly(lactic acid) nanocomposites with silver nanoparticles by spraying method. *Carbohydr Polym* 140:209–219. <https://doi.org/10.1016/j.carbpol.2015.12.030>

**Publisher's Note** Springer Nature remains neutral with regard to jurisdictional claims in published maps and institutional affiliations.